

Random-Multi-Branch Successive Interference Cancellation detection in single-user and multi-user MIMO environments

Alvaro Javier Ortega[†] and Raimundo Sampaio-Neto[‡]

Abstract—This work focuses on a new methodology for use in a Multi-branch Serial Interference Cancellation (MB-SIC) type of MIMO detector. The proposed structure incorporates a low complexity ordering scheme and a variable amount of branches, whose number is controlled by a metric that reflects the quality of the current signal vector estimate. Single and multiple-user environments with both correlated and uncorrelated channels scenarios are considered. Bit error rate results, obtained through simulation, and complexity results, expressed in terms of the required number of flops per detected signal vector, are compared with the corresponding results of previously proposed MB-SIC schemes.

Keywords—MIMO, Multiple Branches SIC, Random Ordering, Variable Number of Branches.

I. INTRODUCTION

Ordering algorithms (e.g., based on the channel norm, the SNR and the SINR) play an important role in the performance of SIC receivers [2]–[4]. A generalization of SIC techniques is the MB-SIC, which employs multiple SIC algorithms in parallel branches producing multiple candidates for detection [5]. The number of parallel branches L is a parameter that must be chosen in the project. In this context, the optimal ordering scheme conducts an exhaustive search $L = N_t!$ (where N_t is the number of transmitted symbols and $!$ is the factorial operator), that means explore all possible different orderings. It is clearly very complex for practical systems, especially when N_t is large. Therefore, an ordering scheme with low complexity is of great interest [6].

The contributions of this paper can be summarized as follows: (i) conclusive results that show that the best option for the ordering pattern in multi-branch detection is a random ordering, without using transformation matrices; (ii) an adaptive detection scheme to choose dynamically an appropriate number of branches at each signal vector detection, resulting in a decrease in complexity; and (iii) comparison of different MB-SIC detectors in terms of performance (i.e., in terms of BER) and complexity (i.e., average account number of flops) in three different scenarios, uncorrelated scenario for single-user MIMO and correlated scenario for multi-user MIMO with centralized and distributed antenna systems.

This work is structured as follows. Section II reviews the system models considered. Section III is dedicated to the description of the considered detection algorithms, which

includes the MB-SIC scheme found in the literature and our proposal named random-multi-branch successive interference cancellation by random order (RMB-SIC-RO). Section IV discusses the results of some simulations. Finally, conclusions are outlined in section V.

II. SYSTEM MODELS

A. Scenario A

Consider a MIMO system with N_t transmit antennas and N_r receive antennas, $N_t \leq N_r$, where N_t symbols are transmitted from N_t transmit antennas simultaneously [7]. Let $\mathbf{s} \in \mathbb{C}^{N_t \times 1}$ be the symbol vector transmitted with the element s_i being the unit energy transmitted complex signal of the i -th user. Let $\mathbf{H} \in \mathbb{C}^{N_r \times N_t}$ be the channel gain matrix, such that the (p, q) -th entry $h_{p,q}$ denotes the complex channel gain from the q -th transmit antenna to the p -th receive antenna. Assuming rich scattering, we model the entries of \mathbf{H} as independent and identically distributed (i.i.d) $\mathcal{CN}(0, 1)$ random variables, where $\mathcal{CN}(0, 1)$ stands for complex gaussian distribution with zero mean and unit variance. Let $\mathbf{r} \in \mathbb{C}^{N_r \times 1}$ and $\mathbf{n} \in \mathbb{C}^{N_r \times 1}$ denote respectively the received signal vector and the noise vector at the receiver, where the entries of \mathbf{n} are modeled as i.i.d $\mathcal{CN}(0, \sigma_n^2)$. The signal-to-noise ratio (SNR) per receiving antenna is defined as $10 \log_{10} \frac{N_t}{\sigma_n^2}$, where σ_n^2 is the noise variance. The received signal vector can be written as

$$\mathbf{r} = \mathbf{H}\mathbf{s} + \mathbf{n} \quad (1)$$

B. Scenario B

In this subsection, we consider a multiuser massive MIMO system with Centralized Antenna System Model (CAS) using N_A antenna elements at the receiver and K users that are equipped with N_U antenna elements each, where $N_A \geq KN_U$ [5], [8]. At each time instant, user k transmits N_U symbols which are organized into a $N_U \times 1$ vector \mathbf{s}_k . The composite received signal after demodulation, pulse-matched filtering and sampling is collected in an $N_A \times 1$ vector \mathbf{r} which can be modeled as

$$\mathbf{r} = \sum_{k=1}^K \gamma_k \mathbf{H}_k \mathbf{s}_k + \mathbf{n} = \sum_{k=1}^K \mathbf{G}_k \mathbf{s}_k + \mathbf{n} = \mathbf{G}\mathbf{s} + \mathbf{n} \quad (2)$$

where $\mathbf{G} = [\mathbf{G}_1 \ \mathbf{G}_2 \ \cdots \ \mathbf{G}_K]$, $\mathbf{s} = [\mathbf{s}_1^T \ \mathbf{s}_2^T \ \cdots \ \mathbf{s}_K^T]^T$, and the entries of $\mathbf{n} \in \mathbb{C}^{N_A \times 1}$

Centre for Telecommunications Research (CETUC) of the Pontifical Catholic University of Rio de Janeiro (PUC-Rio) E-mails: [†] javier.ortega@cetuc.puc-rio.br, [‡] raimundo@cetuc.puc-rio.br

are modeled as i.i.d $\mathcal{CN}(0, \sigma_n^2)$. The data vectors \mathbf{s}_k have zero mean and covariance matrices $\mathbf{E}[\mathbf{s}_k \mathbf{s}_k^H] = \sigma_{s_k}^2 \mathbf{I}$, where $\sigma_{s_k}^2$ is the user k transmit signal power. The elements $h_{i,j}^k$ of the $N_A \times N_U$ channel matrices \mathbf{H}_k are the complex channel gains from the j -th transmit antenna of user k to the i -th receive antenna and using the Kronecker channel model [5], we have that

$$\mathbf{H}_k = \Theta_R^{1/2} \mathbf{H}_k^0 \Theta_T^{1/2} \quad (3)$$

where \mathbf{H}_k^0 has complex channel gains obtained from complex gaussian random variables with zero mean and unit variance, Θ_R and Θ_T denote the receive and transmit correlation matrices, respectively. The components of correlation matrices Θ_R and Θ_T are of the form

$$\Theta_{R/T} = \begin{pmatrix} 1 & \rho & \rho^4 & \dots & \rho^{(N_a-1)^2} \\ \rho & 1 & \rho & \dots & \vdots \\ \rho^4 & \rho & 1 & \vdots & \rho^4 \\ \vdots & \vdots & \vdots & \vdots & \vdots \\ \rho^{(N_a-1)^2} & \dots & \rho^4 & \rho & 1 \end{pmatrix} \quad (4)$$

where ρ is the correlation index of neighboring antennas and N_a is the number of antennas in the transmit or receive array. When $\rho = 0$ we have an uncorrelated scenario and when $\rho = 1$ we have a fully correlated scenario. The parameters $\gamma_k = \alpha_k \beta_k$ represent the large-scale propagation effects for user k such as path loss and shadowing, where the path loss $\alpha_k = \sqrt{\frac{L_k}{d_k^\tau}}$ for each user, L_k is the power path loss of the link associated with user k with respect to the base station, d_k is the relative distance between the user and the base station, τ is the path loss exponent chosen between 2 and 4 depending on the environment.

The log-normal shadowing parameter $\beta_k = 10 \frac{\sigma_k v_k}{10}$, where σ_k is the shadowing spread in dB and v_k corresponds to a random variable $\mathcal{N}(0, 1)$.

C. Scenario C

In this subsection, we consider a multiuser massive MIMO system with a Distributed Antenna System Model (DAS) configuration using: N_B antenna elements at the base station and M remote radio heads each with Q antenna elements, which are distributed over the cell and linked to the base station via wired or optical links, and K users equipped with N_U antenna elements each, where the number of receiving antennas $N_A = N_B + MQ \geq K N_U$ [9]–[14]. Note that if $M = 0$ the DAS architecture reduces to the CAS scheme with $N_A = N_B$.

At each time instant, user k transmits N_U symbols over flat fading channels. In vectorial form we have $\mathbf{s}_k \in \mathcal{C}^{N_U \times 1}$. The composite received signal after demodulation, pulse-matched filtering and sampling is collected in an $N_A \times 1$ vector \mathbf{r} which can be modeled as

$$\mathbf{r} = \sum_{k=1}^K \Gamma_k \mathbf{H}_k \mathbf{s}_k + \mathbf{n} = \sum_{k=1}^K \mathbf{G}_k \mathbf{s}_k + \mathbf{n} = \mathbf{G} \mathbf{s} + \mathbf{n} \quad (5)$$

where $\mathbf{G} = [\mathbf{G}_1 \ \mathbf{G}_2 \ \dots \ \mathbf{G}_K]$, $\mathbf{s} = [\mathbf{s}_1^T \ \mathbf{s}_2^T \ \dots \ \mathbf{s}_K^T]^T$, and the entries of $\mathbf{n} \in \mathbb{C}^{N_A \times 1}$ are modeled as i.i.d $\mathcal{CN}(0, \sigma_n^2)$. The data vectors \mathbf{s}_k have zero mean and covariance matrices $\mathbf{E}[\mathbf{s}_k \mathbf{s}_k^H] = \sigma_{s_k}^2 \mathbf{I}$, where $\sigma_{s_k}^2$ is the user k transmit signal power. The elements $h_{i,j}^k$ of the $N_A \times N_U$ channel matrices \mathbf{H}_k are the complex channel gains from the j -th transmit antenna of user k to the i -th receive antenna. Unlike the CAS architecture, in a DAS setting the channels between remote radio heads are less likely to suffer from correlation due to the fact that they are geographically separated. However, for the antenna elements located at the base station and at each remote radio head, the $M + 1$ submatrices of \mathbf{H}_k are modeled using the Kronecker channel model, so that $\mathbf{H}_k = [\mathbf{H}_{k_1}^T \ \mathbf{H}_{k_2}^T \ \dots \ \mathbf{H}_{k_{M+1}}^T]^T$. The links in the DAS setting experience, in the average, lower path loss effects due to reduced distance between the users and distributed antennas. The large-scale propagation effects are modeled by an $N_A \times N_A$ diagonal matrix given by

$$\Gamma_k = \text{diag} \left[\underbrace{\gamma_{k,1} \dots \gamma_{k,1}}_{N_B} \ \underbrace{\gamma_{k,2} \dots \gamma_{k,2}}_Q \ \dots \ \underbrace{\gamma_{k,M+1} \dots \gamma_{k,M+1}}_Q \right] \quad (6)$$

The parameters $\gamma_{k,j} = \alpha_{k,j} \beta_{k,j}$ for $j = 1, \dots, M + 1$ denote the large-scale propagation effects like shadowing and pathloss from the k -th user to the j -th radio head, where the path loss $\alpha_{k,j} = \sqrt{\frac{L_{k,j}}{d_{k,j}^\tau}}$ for each user and antenna, $L_{k,j}$ is the power path loss of the link associated to user k and the j -th radio head and $d_{k,j}$ distance between them, τ is the path loss exponent chosen between 2 and 4 depending on the environment. The log-normal shadowing $\beta_{k,j} = 10 \frac{\sigma_k v_{k,j}}{10}$, where σ_k is the shadowing spread in dB and $v_{k,j}$ corresponds to a $\mathcal{N}(0, 1)$.

III. COMPARED DETECTORS

The multi-branch successive interference cancellation (MB-SIC) algorithm relies on different ordering patterns to produce multiple candidates for detection. Each ordering is referred to as a branch, so that a detector with L branches produces a set of L estimated vectors. Then the MB-SIC algorithm selects the candidate branch with the minimum Euclidean distance.

The ordering of the first branch is identical to a standard SIC algorithm and could be based on the channel norm, *signal-to-noise-ratio* (SNR) or the *signal-to-interference-plus-noise-ratio* (SINR), which is the best option; while, the remaining branches are ordered by shifted orderings relative to the first branch. This paper considers SINR ordering, that is signals with higher SINR values are detected first [2], [3]. Considering MMSE linear detection, the i -th symbol detected is

$$\hat{\mathbf{s}}_i = Q (\mathbf{w}_i^H \mathbf{r}), \quad i = 1, 2, \dots, N_t \quad (7)$$

where \mathbf{w}_i is the i -th column of the MMSE detection matrix given by $\mathbf{W}_{MMSE} = \mathbf{H} (\mathbf{H}^H \mathbf{H} + \sigma_n^2 / \sigma_s^2 \mathbf{I})^{-1}$ and

the function $Q(x)$ returns the point of the complex signal constellation closest to x . The SINR in the i -th symbol is

$$SINR_i = \frac{E_{s_i} |\mathbf{w}_i^H \mathbf{h}_i|^2}{\sum_{l=1, l \neq i}^{N_t} E_{s_l} |\mathbf{w}_i^H \mathbf{h}_l|^2 + \sigma_n^2 \|\mathbf{w}_i\|^2} \quad (8)$$

for $i = 1, 2, \dots, N_t$, \mathbf{h}_l ($l = 1, 2, \dots, N_t$) is the l -th column of the channel matrix \mathbf{H} and E_{s_i} is the energy of the transmitted symbol s_i . N_t values of SINR are calculated and ordered from highest to lowest, then the N_t symbols are detected following this same order.

Subsections III-A and III-B describe a methodology for reordering the remaining branches by permutation and in a random fashion, respectively, both using a fixed number of branches. The subsection III-C defines a new methodology based in [15] where the ordering patterns are randomly chosen but the number of branches is variable.

A. Multi-Branch Successive Interference Cancellation by Permutation Order (MB-SIC-PO)

In this algorithm each branch uses a column permutation matrix \mathbf{P} . The estimate of the signal vector of l -th branch, $\hat{\mathbf{x}}_l$, is obtained using a SIC receiver based on a new channel matrix $\mathbf{H}^{(l)} = \mathbf{H}\mathbf{P}_l$ [16]. The order of the estimated symbols is rearranged to the original order by

$$\hat{\mathbf{s}}_l = \mathbf{P}_l \hat{\mathbf{x}}_l, \quad l = 1, \dots, L \quad (9)$$

According to [16] the permutation matrix is described by

$$\mathbf{P}_l = \begin{bmatrix} \mathbf{I}_s & \mathbf{0}_{s, N_t-s} \\ \mathbf{0}_{N_t-s, s} & \bar{\mathbf{I}}_{N_t-s} \end{bmatrix}, \quad 2 \leq l \leq L \quad (10)$$

where \mathbf{I}_m is an identity matrix of size $m \times m$, $\mathbf{0}_{m,n}$ denotes $m \times n$ -dimensional matrix full of zeros and $\bar{\mathbf{I}}_m$ represents a reversal matrix $m \times m$.

The algorithm shifts the ordering of the cancellation according to shifts given by

$$s = \lfloor (l-2)N_t/L \rfloor, \quad 2 \leq l \leq N_t \quad (11)$$

where L is the number of parallel branches and $\lfloor \cdot \rfloor$ rounds the argument to the lowest integer according to the l -th branch. Expressions (10) and (11) evidence can be seen that the maximum number of branches is equal to the number of transmit antennas, $L \leq N_t$.

B. Multi-Branch Successive Interference Cancellation by Random Order (MB-SIC-RO)

This scheme is very simple, the ordering in the first branch is made according to a standard SIC algorithm while the remaining branches employ an ordering vector \mathbf{i}_l (where the subindex l represents the corresponding branch, $l = 2, \dots, L$) formed by integers between 1 and the number of symbols transmitted N_t , randomly selected without replacement.

C. Random-Multi-Branch Successive Interference Cancellation by Random Order (RMB-SIC-RO)

In this subsection a new detection scheme is presented. Our proposal is a variation of the RLB-LAS [15]. Similarly to the detector MB-SIC-RO, the main idea of the algorithm RMB-SIC-RO is to generate several estimates of the transmitted signal vector through SIC detectors with different orderings. However, here the number of branches, L , which corresponds to the number of candidates tested for each received signal vector, is variable and depends on a stopping criterion.

The RMB-SIC-RO detector is summarized in the Algorithm 1. The input and output of this algorithm is \mathbf{r} and $\hat{\mathbf{s}}_{opt}$, respectively. The ordering in the first branch, \mathbf{i}_s , is done according to a standard SIC algorithm while the remaining branches employ the random ordering vector, \mathbf{i}_l . The function "SIC" represents the SIC detector and has as inputs: the input vector \mathbf{r} , the channel matrix \mathbf{H} and the ordering vector; and has as output: the Maximum Likelihood (ML) cost value, C_{ml} , of the estimated vector and the estimated vector of transmitted symbols $\hat{\mathbf{s}}$. Note that the first estimate is considered as $\hat{\mathbf{s}}_{opt}$ but in the course of the algorithm it may be replaced by a better estimate (e.g., with a lower value of the ML cost function). The stopping criterion defines a number of iterations N_p which depends on the value of the ML cost function of the best estimate, $C_{ml_{opt}}$. The "stopcriterion" function gives the value of N_p [15], which is calculated as follows,

$$N_p = \lceil \max(c\phi(\hat{\mathbf{s}}), N_{p_{min}}) \rceil \quad (12)$$

where c is a constant, the operator $\lceil a \rceil$ gives the largest integer less than a , $N_{p_{min}}$ sets the minimum number of iterations and $\phi(\hat{\mathbf{s}})$ is given by

$$\phi(\hat{\mathbf{s}}) = \frac{2C_{ml}(\hat{\mathbf{s}}) - N_t\sigma_n^2}{\sqrt{N_t}\sigma_n^2} \quad (13)$$

and $C_{ml}(\hat{\mathbf{s}}) = \|\mathbf{r} - \mathbf{H}\hat{\mathbf{s}}\|^2$ is the ML cost function.

At the end of each iteration, if the iteration number is greater than N_p , the algorithm stops and the current decision signal vector is elected as the final detected signal vector.

Algorithm 1: RMB-SIC-RO

```

input :  $\mathbf{r}$ 
output:  $\hat{\mathbf{s}}_{opt}$ 
1  $[C_{ml_{opt}}, \hat{\mathbf{s}}_{opt}] = \text{SIC}(\mathbf{r}, \mathbf{H}, \mathbf{i}_s)$ 
2  $N_p = \text{stopcriterion}(C_{ml_{opt}})$ 
3 iteration = 0
4 while iteration <  $N_p$  do
5     iteration = iteration + 1
6      $[C_{ml}, \hat{\mathbf{s}}_l] = \text{SIC}(\mathbf{r}, \mathbf{H}, \mathbf{i}_l)$ 
7     if  $C_{ml} < C_{ml_{opt}}$  do
8          $C_{ml_{opt}} = C_{ml}$ 
9          $\hat{\mathbf{s}}_{opt} = \hat{\mathbf{s}}_l$ 
10         $N_p = \text{stopcriterion}(C_{ml_{opt}})$ 
11    end
12 end
    
```

IV. NUMERICAL RESULTS

We consider 4-QAM modulation, data packets of 10^2 symbols, fixed channels during each transmitted data packet, perfect channel state information and synchronization. The numerical results are averaged over 10^3 runs. Each of the MB-SIC detectors use linear MMSE receiver filters and ordering by SINR for the first branch. RMB-SIC-RO parameters used in the simulation are $N_{pmin} = 2$ and $c = 5$, these values were taken from the detector RLB-LAS in [15]; however, it is necessary to make a proper study for the proper selection of these parameters, because they compromise the complexity and performance of the detector. Moreover, the fixed number of branches is equal to the number of transmit antennas, $L = N_t$. For the CAS configuration, we employ $L_k = 0.7$, $\tau = 2$, the distance d_k to the BS is obtained from a uniform discrete random variable between 0.1 and 0.95, the shadowing spread is $\sigma_k = 3$ dB and the transmit and receive correlation coefficients are equal to $\rho = 0.2$. The SNR in dB per receive antenna is given by $SNR = 10 \log_{10} \frac{K N_U \sigma_{s_r}^2}{\sigma_n}$, where $\sigma_{s_r}^2 = \sigma_{s_k}^2 E[|\gamma_k|^2]$ is the variance of the received symbols. $N_A = 32$ antenna elements at the receiver, $K = 16$ users and $N_U = 2$ antenna elements at the user devices is considered. For the DAS configuration, we use $L_{k,j}$ taken from a uniform random variable between 0.7 and 1, $\tau = 2$, the distance d_k is obtained from a uniform discrete random variable between 0.1 and 0.5, the shadowing spread is $\sigma_k = 3$ dB and the transmit and receive correlation coefficients are equal to $\rho = 0.2$. The SNR in dB per receive antenna is given by $SNR = 10 \log_{10} \frac{K N_U \sigma_{s_r}^2}{\sigma_n}$, where $\sigma_{s_r}^2 = \sigma_{s_k}^2 E[|\gamma_{k,j}|^2]$ is the variance of the received symbols. $N_A = N_B + LQ = 32$ antenna elements processed at the receiver with $M = 16$ remote radio heads each with $Q = 1$ antenna elements, $K = 16$ users and $N_U = 2$ antenna elements at the user devices is considered.

Figures 1 and 2 show the results of performance and complexity, respectively, of the considered detectors for 8x8, 20x20 and 32x32 systems in scenario A, where the configuration in this case is $N_t = N_r$ for $N_t = 8$, $N_t = 20$ and $N_t = 32$, respectively. It can be seen that in all cases the BER performance curves of the proposed RMB-SIC-RO detector remains below the other curves and that the MB-SIC detector achieves a performance similar to the RMB-SIC-RO only for the 32x32 system but with higher complexity.

Figures 3 and 4 show the results of performance and complexity, respectively, of the focused detectors operating in scenarios B and C with modulation 4-QAM. Note that in those scenarios the performance of the detectors resulted very similar. The real advantage of our proposal for these scenarios is the complexity. Note that for detectors MB-SIC-PO and MB-SIC-RO the number of flops remains constant and independent of the type of scenario. On the other hand, the performance in terms of complexity of the proposed RMB-SIC-RO varies and is clearly dependent of the type of scenario. It is worthy noting that the average number of flops per detected signal vector required by RMB-SIC-RO detector tends to grow with increasing SNR, and that makes sense, the quality of the initial candidate improves with an increasing SNR, and the better is the initial candidate, the larger, in the

average, is the number of candidates that have to be tested before finding a better one.

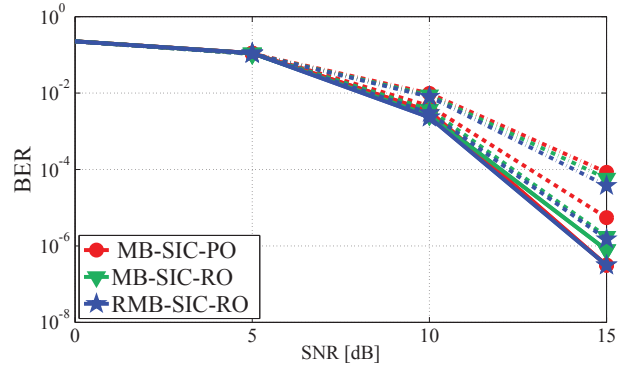


Fig. 1

PERFORMANCE OF MB-SIC-PO, MB-SIC-RO AND RMB-SIC-RO DETECTORS IN 8x8 (· · ·), 20x20 (— —) AND 32x32 (—) SYSTEMS WITH MODULATION 4-QAM IN THE SCENARIO A

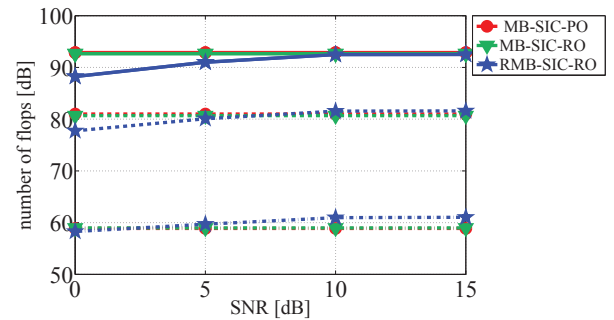


Fig. 2

COMPLEXITY OF MB-SIC-PO, MB-SIC-RO AND RMB-SIC-RO DETECTORS IN 8x8 (· · ·), 20x20 (— —) AND 32x32 (—) SYSTEMS WITH MODULATION 4-QAM IN THE SCENARIO A

V. CONCLUSION

This article has presented a comparison of three types of MB-SIC detectors, two of them proposed here. A low complexity MB system that uses a variable number of branches, controlled by a stopping criterion was introduced. We consider three different scenarios for a broader vision and comparison of the considered detector strategies. Numerical results and comparisons have indicated a superiority in BER performance of the proposed MB-SIC-RO detector over the other two, without an increase in complexity, an even with lower complexity in some scenarios.

The use of a variable number of branches, whose number is controlled by a function of the ML cost of the current best solution, as in the RLB-las and RMB-SIC-RO detectors, has shown to be a good strategy in the search for efficient MB detection techniques. It is to be noted, however, that the number of branches determined by the stopping criterion,

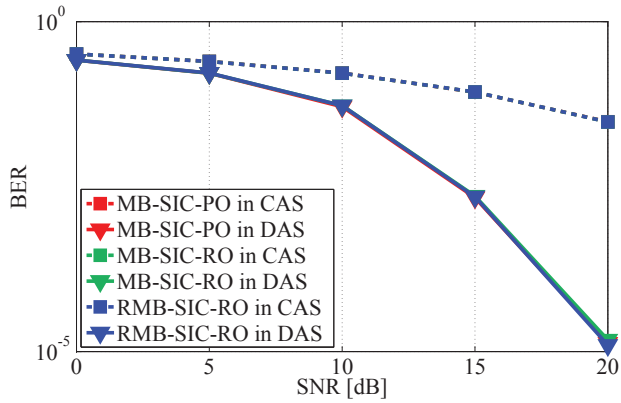


Fig. 3

PERFORMANCE OF MB-SIC-PO, MB-SIC-RO AND RMB-SIC-RO DETECTORS WITH MODULATION 4-QAM, $K = 16$ AND $N_U = 2$ IN THE SCENARIOS B AND C

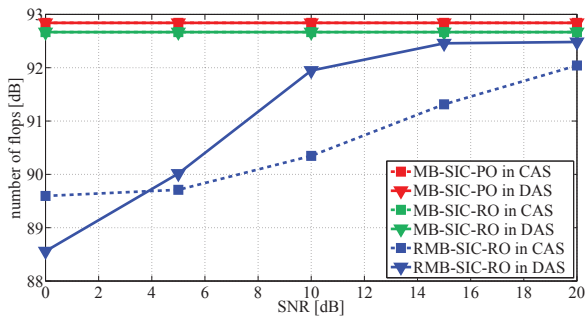


Fig. 4

COMPLEXITY OF MB-SIC-PO, MB-SIC-RO AND RMB-SIC-RO DETECTORS WITH MODULATION 4-QAM, $K = 16$ AND $N_U = 2$ IN THE SCENARIOS B AND C

described in Subsection III-C, is dependent of parameters such as the constants c and $N_{p_{min}}$ in (12). A proper (or optimal, if possible) choice of these parameter can improve further the trade-off performance versus complexity and certainly is an interesting topic for future research.

REFERENCES

- [1] J. Chen, F. Telebi, and T. Pratt, *Energy Efficiency of Co-polarized and Space-Polarization MIMO Architectures in Packet-Based Communication Systems*, Military Communications Conference, MILCOM 2013-2013 IEEE, IEEE, 2013, pp. 311-316.
- [2] A. A. Minhas, K. Shabir, I. Mehmood, and A. Al Mazyad, *Layers ordered multiple feedback successive interference cancellation in MU-MIMO in High Capacity Optical Networks and Enabling Technologies (HONET-CNS)*, 2013 10th International Conference on. IEEE, 2013, pp. 214-218.
- [3] M. Mohammad and R. M. Buehrer, *The effects of ordering criteria in linear successive interference cancellation in CDMA systems*, Wireless Communications, IEEE Transactions on, vol. 7, no. 11, pp. 4128-4132, 2008.
- [4] A. Zanella, M. Chiani, and M.Z. Win, *MMSE reception and successive interference cancellation for MIMO systems with high spectral efficiency*, Wireless Communications, IEEE Transactions on, vol. 4, no. 3, pp. 1244-1253, 2005.

- [5] R.C. De Lamare and R. Sampaio-Neto, *Signal detection and parameter estimation in massive MIMO systems*, in Signals and Images: Advances and Results in Speech, Estimation, Compression, Recognition, Filtering and processing. CRC Press, Chapter 13, 2015.
- [6] R. Fa and R. C. De Lamare, *Multi-branch successive interference cancellation for MIMO spatial multiplexing systems: design, analysis and adaptive implementation*, IET communications, vol.5. no. 4, pp. 484-494, 2011.
- [7] X. Zhu and R.D. Murch, *Performance analysis of maximum likelihood detection in a MIMO antenna systems*, Communications, IEEE Transactions on, vol. 50. no. 2, pp. 187-191, 2002.
- [8] D.S. Russell, L.G. Fischer, and P.M. Wala, *Cellular communications system with centralized base stations and distributed antenna units*, Aug. 12 1997, uS Patent 5,657,374.
- [9] A. J. Powell, *Distributed antenna systems*, Apr. 10 1990, uS Patent 4,916,460.
- [10] W. Roh and A. Paulraj, *MIMO channel capacity for the distributed antenna*, in Vehicular Technology Conference, 2002. Proceedings. VTC 2002-Fall. 2002 IEEE 56th, vol 2. IEEE, 2002, pp. 706-709.
- [11] H. Zhuang, L. Dai, L. Xiao, and Y. Yao, *Spectral efficiency of distributed antenna system with random antenna layout*, Electronic Letters, vol. 39, no. 6, pp 495-496, 2003.
- [12] D. Castanheira and A. Gameiro, *Distributed antennas systems caacity scaling [coordinated and distributed MIMO]*, Wireless Communications IEEE, vol. 17, no. 3, pp. 68-75, 2010.
- [13] J. C. Guey and K. C. Zangi, *Distributed antenna systems*, Jan. 21 2014, uS Patent 8,634,357.
- [14] M. Shida, *Distributed antenna systems*, Dec. 30 2014, uS Patent 8,923,908.
- [15] A. A. Pereira Jr. and R. Sampaio-Neto, *A Random-List Based LAS Algorithm for Near-Optimal Detection in Large-Scale Uplink Multiuser MIMO Systems*, in WSA 2015; 19th International ITG Workshop on Smart Antennas; Proceeding of. VDE, 2015, pp. 1-5.
- [16] L. Arévalo, R. C. De Lamare, K. Zu, and R. Sampaio-Neto, *Multi-branch lattice reduction successive interference cancellaion detection for multiuser MIMO systems*, in Wireless Communications Systems (ISWCS), 2014 11th International Symposium on. IEEE, 2014, pp. 219-223.